

Thesis/
Reports
Claessens

THE COMPLEMENTARY RELATIONSHIP IN
REGIONAL EVAPOTRANSPIRATION:

Lodevicus H. J. M. Claessens

February

THE COMPLEMENTARY RELATIONSHIP IN REGIONAL EVAPOTRANSPIRATION: EVALUATION OF MORTON'S CRAE MODEL USING LONG-TERM LARGE-SCALE WATER BALANCES

Lodevicus H.J.M. Claessens¹ and Jorge A. Ramirez
Department of Civil Engineering
Colorado State University
Fort Collins

Thomas C. Brown
Rocky Mountain Research Station
USDA Forest Service
Fort Collins, Colorado

Final Report
Cooperative Agreement 28-C2-618
Large Scale Water Budgets for the U. S.

between
Colorado State University
and
Rocky Mountain Research Station

September 1997

¹ Currently at the Ecosystems Center, Marine Biological Laboratory, Woods Hole, MA.

In addition to the following report, the work completed under cooperative agreement 28-C2-618 is documented in the thesis by Luc Claessens titled "The Complementary Relationship in Regional Evapotranspiration and Long-term Large-scale Water Budgets," submitted to the Department of Civil Engineering of Colorado State University in the Fall of 1996.

ABSTRACT

Bouchet's hypothesis of a complementary relationship between actual and potential regional evapotranspiration is based on the interactive nature of evaporative processes. Morton's implementation of this hypothesis, the Complementary Relationship Areal Evapotranspiration (CRAE) model, is evaluated against independent estimates of regional evapotranspiration derived from long-term large-scale water balances (1962-1988), for minimally impacted basins in the conterminous USA, east of the Continental Divide. Water balance residuals were calculated as precipitation minus streamflow minus CRAE evapotranspiration. The results indicate an overall excellent performance of the CRAE model. Average water balance residuals, when expressed as percent of average annual precipitation, were negative and generally small, with an average value of -1.7 percent. Regions with low annual precipitation displayed large negative residuals, which could be associated with violation of minimum impact assumption, through the influence of irrigated agriculture. In addition, regions with high moisture availability displayed large negative residuals as well, suggesting overprediction of CRAE model evapotranspiration for these regions. The largest basin (308,210 km²; Mississippi river at Keokuk, Iowa) had an average annual water balance residual of only -5.2 mm. Overall, the results indicate that the CRAE model is a powerful tool for predicting regional evapotranspiration.

1. INTRODUCTION

One of the most challenging problems in hydrometeorology is that of describing the spatial variability of geomorphoclimatic forcing and its effects on hydrometeorologic fluxes. Our apparently sound understanding of the small scale physics cannot be applied directly to understand large scale behavior. In problems of global climate or even regional hydrology, understanding the large scale behavior of processes that define sensible and latent heat fluxes is of paramount importance. If, in addition to the spatial scale, temporal scales ranging from very small to very large are considered, the problems are compounded by the potential feedback interactions between the land surface and the atmosphere.

In hydrology it has been customary to use empirical relationships for the description of large scale fluxes. In particular, actual evapotranspiration usually has been modeled as a function of both potential evapotranspiration and soil moisture availability. Potential evapotranspiration is often considered an independent climatic variable, and feedback mechanisms linking atmospheric and land surface fluxes are ignored.

Yet, it has long been recognized that actual and potential evapotranspiration are not independent of each other [*Bouchet*, 1963]. Complex feedback interactions between processes governing the rates of actual and potential evapotranspiration are established based on the degree to which the soil can satisfy the atmospheric demand for water vapor and on the resultant effect on the energy distribution at the land-atmosphere interface, especially at regional scales. *Bouchet* [1963] hypothesized a mutual, complementary dependence structure between actual and potential evapotranspiration, which led to the development of several so-called *complementary relationship* models. The most widely known models are the Complementary Relationship Areal Evapotranspiration (CRAE) model [*Morton*, 1965, 1983] and the Advection-Aridity model [*Brutsaert and Stricker*, 1979].

Apart from Morton's numerous publications, several studies have addressed the validity of complementary relationship models, whether through comparison among other evapotranspiration

estimators [Ben-Asher, 1981; Sharma, 1988; Doyle, 1990; Lemeur and Zhang, 1990; Chiew and McMahon, 1991; Parlange and Katul, 1992a], analysis based on meteorological observations and/or modeling results [LeDrew, 1979; McNaughton and Spriggs, 1989; Granger and Gray, 1990; Lhomme, 1997; Kim and Entekhabi, 1997] or by defining improvements to existing models [Kovacs, 1987; Granger, 1989; Parlange and Katul, 1992b]. Although complementary relationship models have been evaluated with varied success, the complementary relationship hypothesis is considered an important concept for hydrologic modeling [Nash, 1989; Dooge, 1992].

Since none of the above studies evaluated the complementary relationship over a wide range of climatologically varying conditions (e.g., continental size areas), its value as an operational tool for hydrologic modeling has not been well established. Therefore, in this study we evaluated Morton's CRAE model [Morton, 1983; Morton *et al.*, 1985] against independent estimates of actual evapotranspiration derived from long-term large-scale water balances for minimally impacted basins in the conterminous USA east of the Continental Divide.

2. THE COMPLEMENTARY RELATIONSHIP

Bouchet's hypothesis of a complementary relationship states that, for areas of regional size, there exists a mutual dependence structure, or feedback mechanism, between actual and potential evapotranspiration of a complementary nature. In this context, potential evapotranspiration is defined as the evapotranspiration that would take place from a moist surface under the prevailing atmospheric conditions, limited only by the amount of available energy. At conditions where actual evapotranspiration (ET_a) equals potential evapotranspiration (ET_p), the evapotranspiration is sometimes referred to as the wet environment evapotranspiration (ET_w). The general complementary relationship is then given by:

$$ET_a + ET_p = 2ET_w. \quad (1)$$

This complementary relationship is illustrated in Figure 1, where under conditions of constant energy supply, the actual and potential evapotranspiration components sum to twice the value of the wet environment evapotranspiration.

The complementary relationship hypothesis was essentially based on empirical observations, supported by a conceptual description of the underlying processes that control the complementary behavior between actual and potential evapotranspiration. Heuristically, when actual evapotranspiration falls below its potential due to water limitations, a certain amount of energy becomes available. This energy excess, in the form of sensible heat and/or long wave back radiation, then changes the value of ET_p . Bouchet hypothesized that the increase in potential evapotranspiration is equal in amount to the decrease in actual evapotranspiration. As such, potential evapotranspiration ceases to be an independent causal factor, or climatologically constant forcing function, and becomes a dependent quantity determined by the particular conditions of moisture availability.

Underlying Bouchet's hypothesis is an interaction between evapotranspiring surfaces and the over-passing air. Changes in the availability of water for actual evapotranspiration lead to changes in the temperature and humidity gradients of the atmospheric boundary layer, which in turn lead to changes in potential evapotranspiration. Local temperature and humidity gradients of the atmospheric boundary layer respond to and are a reflection of the conditions of moisture availability at the surface. As such, the main advantage of methods based on Bouchet's hypothesis is that no soil moisture data are required.

3. METHODOLOGY

3.1 The CRAE Model

As indicated above, several models have been developed that incorporate Bouchet's hypothesis of a complementary relationship. All of these complementary relationship models share the same conceptualization of potential evapotranspiration and regional advection. Potential evapotranspiration is calculated by combining information from the energy budget and water vapor transfer, and wet environment evapotranspiration is calculated based on the concept of equilibrium evapotranspiration under conditions of minimal advection.

In this study, the Complementary Relationship Areal Evapotranspiration (CRAE) model [Morton, 1983; Morton *et al.*, 1985] was used to obtain independent estimates of regional actual evapotranspiration. Details on the concept of potential evapotranspiration and regional advection are presented in Appendix A. Computational specifics of the CRAE model are presented in Appendix B.

3.2 The Water Balance

The water balance for a basin during a period Δt can be described in a lumped or averaged hydrologic system as

$$ET_a = P - R - R_g - D - \Delta S_u - \Delta S_s - \Delta S_g, \quad (2)$$

where each term is an equivalent volume of liquid water and the symbols are defined as follows: ET_a is actual evapotranspiration; P is precipitation; R is net streamflow out of the basin; R_g is net groundwater discharge out of the basin; D is the net volume of water diverted from the basin; ΔS_u is change of storage in the unsaturated zone; ΔS_s is change of storage in surface water (including snowpack); and ΔS_g is change in groundwater storage. The components that can be readily quantified are precipitation, surface discharges to and from the basin, water diversions to and from the basin, and change in storage of surface water.

Water balances can be used for estimating evapotranspiration only for time scales over which the storage changes are zero or known with some degree of certainty. Assuming stationarity conditions for the climatic forcing, the long-term (i.e., climatological), large-scale water balance for an undisturbed basin should lead to negligible net changes in overall basin moisture storage. If net groundwater flow out of the basin is also negligible, the long-term large-scale water balance can be simplified as

$$P = ET_a + R. \quad (3)$$

Thus, an estimate of the long-term average annual evapotranspiration can be obtained from data on precipitation and streamflow. This estimate can then be compared with the long-term average annual value as obtained from monthly evapotranspiration estimates using the CRAE model. As such, the long-term large-scale water balance provides a means to evaluate the performance of the CRAE model.

3.3 Data Sets

The following data sets were used to obtain long-term estimates of streamflow, precipitation and evapotranspiration.

Streamflow: “A Daily Hydroclimatological Data Set for the Continental United States” [Wallis *et al.*, 1991] and the U.S. Geological Survey (USGS) “Hydro-Climatic Data Network (HCDN)” [Slack and Landwehr, 1992]. These two data sets include only those basins with little or no regulation, and include corrections for missing values and station relocations. Between them they contain data for about 1,475 gaging stations. Both data sets cover the water years 1948 through 1988.

Precipitation and Temperature: “Summary of the Day” [EarthInfo, 1993]. This data set contains long-term records of NOAA-NWS and cooperative stations. There are about 13,000 stations in the

conterminous USA. The data record for some stations goes back as far as 1900 and is updated continuously.

Solar Radiation: “Solar and Meteorological Surface Observation Network (SAMSON)” [NREL, 1992]. This data set contains both observed solar radiation from first-order weather stations and modeled solar radiation for selected second-order weather stations, totaling 215 stations in the conterminous USA. The data record covers the period 1961 through 1990.

Humidity: “Surface Airways” [EarthInfo, 1993]. This data set contains long-term records of dewpoint temperature for first and second order NWS stations. There are 323 stations in the conterminous USA. The data record for most stations starts in 1948 and is updated continuously.

Albedo: an update from the Gutman [1988] average monthly albedo surfaces [G. Gutman, personal communication, 1995]. This data set contains AVHRR derived albedo estimates, with a resolution of about 15 km.

Elevation: a 30-arc second DEM (NOAA-NGDC).

Based on the record lengths of the available data sets we confined our study to the water years 1962-1988.

3.4 Spatial Interpolation

In order to obtain areal surfaces of precipitation and evapotranspiration, a spatial interpolation technique must be applied to the point observations of meteorological variables. Because the observation networks for both solar radiation and humidity are very sparse, the use of an inverse distance weighted (IDW) method was deemed adequate, using the IDW model parameters $b=2$ (inverse square distance) and $n=12$ (number of points used in interpolation).

For mountainous regions, orographic effects greatly influence areal precipitation patterns, making the IDW scheme inappropriate, as it does not account for factors other than distance. PRISM (Precipitation-elevation Regressions on Independent Slopes Model) [Daly *et al.*, 1994] has been especially designed for these conditions. PRISM estimates the distribution of precipitation by performing linear precipitation-elevation regressions for topographic facets of similar aspect. At

the time of our study, only average monthly surfaces (1961-1990) were available using PRISM. Comparison of an IDW generated average annual precipitation surface (1962-1988) to the annual PRISM surface is presented in Figure 2. The most significant differences are in the western USA. These differences are the result of the applied method of interpolation and possibly the incorporation of the SNOTEL data set in the PRISM scheme, resulting in relatively higher estimates of areal precipitation at very high elevations [Dolph and Marks, 1992]. Overall, the difference between IDW and PRISM for the region east of the Continental Divide is within +/- 5 percent.

Claessens [1996] presented results from cross-validation analysis, testing simple and improved IDW spatial interpolation schemes for solar radiation, temperature and humidity. It was shown that spatial interpolation of average temperature could be improved by incorporating a simple adiabatic adjustment into the IDW scheme. The adiabatic adjustment consists of three steps: 1) transforming the temperature values to potential temperature (potential temperature is the temperature that a mass of air would have if it were compressed or expanded adiabatically to a pressure of 1000 mbar); 2) carrying out the spatial interpolation on the transformed data set; and 3) reversing the potential temperature transformation. An adiabatic adjustment was also applied to dewpoint temperature, improving the performance of the IDW scheme. An additional interpolation scheme was tested for dewpoint temperature by combining gridded minimum temperature surfaces (derived from "Summary of the Day" data), with interpolated surfaces of the difference between minimum temperature and dewpoint temperature ($T_{min}-T_{dew}$) (derived from "Surface Airways" data). This modified IDW approach attempted to preserve the regional characteristics of the relationship between dewpoint temperature and minimum temperature, while making use of the denser network of temperature observations. However, this scheme gave poor performance, primarily due to the high level of spatial heterogeneity in the ($T_{min}-T_{dew}$) surfaces. Consequently, the simpler adiabatic adjusted IDW scheme was adopted in this study for both average temperature and dewpoint temperature.

3.5 Determination of Grid Cell Size

An important consideration in performing grid-based large-scale water balances is the spatial resolution of the analysis window. In order to obtain a justified balance between accuracy and computational constraints, an analysis was performed of the effect of grid cell size on accuracy, using a 3 km grid as the baseline estimate. Gridded precipitation and evapotranspiration surfaces were constructed for the month of July, 1978, with grid cell length-scales ranging from 3 km to 32 km. Integration of the estimation error surfaces over representative areas (i.e., USGS 8-digit hydrologic units) resulted in probability distribution plots for the two variables (Figure 3). Within these plots, each line represents a 5th percentile. The three bold lines refer to the 5th, 50th and 95th percentiles of each distribution at the corresponding grid cell resolution.

The deflection point in these plots is helpful in selecting the "optimal" grid cell size. The graphical analysis for both evapotranspiration and precipitation indicates that a grid cell size of 10 km offers a reasonable balance between accuracy and computational constraints. Larger grid cell sizes result in an unacceptable increase in the variance of the distribution of the estimation error, whereas smaller grid cell sizes result in excessive additional computational burden with only a relatively minor decrease of the estimation error variance. Compared to precipitation, evapotranspiration displays a more clearly defined deflection point, which should be expected, since the evapotranspiration estimation error reflects the combined estimation errors from all the inputs to the evapotranspiration estimation (i.e., temperature, solar radiation, humidity, albedo and elevation).

3.6 Basin Selection and Network

In regions of strong orographic contrast within the conterminous USA, IDW interpolation performed poorly in modeling the spatial representation of meteorological point observations [Claessens, 1996]. Precipitation surfaces were especially poorly presented (Figure 2). Because precipitation is a major component of the water balance, regions of complex terrain were generally

excluded from this study. Consequently, the study area was confined to the region east of the Continental Divide.

Minimally impacted basins were selected in order to perform a long-term analysis of the water balance components, as well as for purposes of evapotranspiration model verification. Only basins that are incorporated in the data sets "A Daily Hydroclimatological Data Set for the Continental United States" [Wallis *et al.*, 1991] and the USGS "Hydro-climatic Data Network (HCDN)" [Slack and Landwehr, 1992] were considered. In addition to having a relatively low level of intra-basin diversion, Ramírez and Claessens [unpublished report, 1994] concluded, based on two USGS inter-basin transfer inventories [Petsch, 1985; and Mooty and Jeffcoat, 1986], that the basins in this study were only minimally affected by inter-basin diversions.

Because at the time of this study there did not exist a comprehensive digital data set on USGS gaged watershed boundaries, we used the digital delineation of the USGS 8-digit Hydrologic Unit Codes (HUC), combined with published sizes of gage drainage areas. Only gages for which the associated HUCs constituted from 85 percent to 115 percent of the gage drainage area were considered. Over the entire study area, 164 basins were selected, based on criteria of minimum impact and the 85-115 percent range (Figure 4). The 164 basins contain a total of 363 HUCs. For this study, a basin was classified either as of first-order or as of higher-order, where the order reflects the number of HUCs associated with the larger basin. Eighty-seven of the basins are labeled as first-order and the remaining 77 as higher-order. The basins cover approximately 25 percent of the total area of study. Table 1 classifies the selected basins by size.

For a higher-order basin, the streamflow for each component HUC was estimated by applying a simple network analysis, which preserved the streamflow volume of the lower-order basins contained in the higher-order basin. The local streamflow volume for each HUC was calculated as a weighted value of the total streamflow volume for the entire basin. The corresponding weighting factor was calculated as the ratio of local volume of precipitation minus evapotranspiration (of the lower-order basin) to the total volume of precipitation minus evapotranspiration for the higher-order basin. For those cases where evapotranspiration exceeded precipitation, the calculations

were carried out in an aggregated basis for the entire basin, resulting in one single value of water balance residual (i.e., precipitation minus streamflow minus evapotranspiration) representing the aggregation of the component HUCs.

4. RESULTS

4.1 Spatial Patterns of the Main Water Balance Components

For the 27 years of record (1962-1988), monthly surfaces were constructed for solar radiation, dewpoint temperature and average temperature. These surfaces were used as input to the CRAE model, resulting in monthly surfaces of wet environment evapotranspiration, potential evapotranspiration and actual evapotranspiration.

Average annual surfaces of wet environment evapotranspiration, potential evapotranspiration, actual evapotranspiration and precipitation are presented in Figure 5. Wet environment evapotranspiration (Figure 5a) has a strong latitudinal gradient, a direct result of the latitudinal gradient in radiative forcing. Potential evapotranspiration (Figure 5b) displays a similar gradient, but is also influenced in the western region by the decrease in precipitation (Figure 5d), resulting in a limitation of moisture supply and subsequent decrease in actual evapotranspiration (Figure 5c) and increase in potential evapotranspiration.

Figure 6 presents the average annual surface of the difference between precipitation and actual evapotranspiration, both in absolute units (mm) and in relative units (percentage of average annual precipitation). This difference represents the average annual net basin yield including contributions from surface runoff, interflow and groundwater discharge/recharge. Areas can be distinguished where predicted evapotranspiration exceeds precipitation, which might be an indication of groundwater depletion, surface water diversions into the area, net streamflow into the area, non-stationarity in climatological forcing, under-prediction of precipitation or over-prediction of evapotranspiration. In southern Texas and in several regions along the Rocky Mountain front

range, this difference between evapotranspiration and precipitation amounts to more than 30 percent of the average annual precipitation.

4.2 Water Balance Residual Analysis

For each of the 164 basins, average annual values were obtained for precipitation, streamflow, actual evapotranspiration and water balance residual. The water balance residual (or evapotranspiration estimation error) is defined as the spatially averaged precipitation minus observed streamflow minus predicted (i.e., estimated using CRAE model) evapotranspiration. A water balance residual different from zero can be an indication of: (i) violation of the assumption of undisturbed conditions, through the effect of groundwater pumping and/or surface-water diversions; (ii) violation of the assumption of stationarity in climatological forcing; (iii) violation of the assumption of negligible net groundwater flow out of the basin; (iv) errors in the hydroclimatological record (including errors induced by spatial interpolation); and (v) either an overprediction (negative residual) or underprediction (positive residual) of evapotranspiration by the CRAE evapotranspiration estimate.

Figure 7 presents the spatial distribution of the water balance residuals, both in absolute units (mm) and in relative units (percentage of average annual basin precipitation). The values of water balance residual are generally small in the Midwest and in the Coastal Plains (+/- 4 percent of average annual precipitation). Negative residuals can be observed in the Appalachian Mountains Region, extending from northern Georgia north-northeastward to northwestern Maine, with large negative residuals in northern Maine. Residuals tend to become more negative when moving westward from the Midwest. Because in this region streamflow constitutes only a minor component of the water balance, the distribution of the water balance residual is very similar to that of the average annual surface of precipitation minus evapotranspiration (Figure 6). The negative residuals in the Northern Great Plains and southern Texas could be a direct result of the effect of irrigated agriculture, through groundwater depletion and surface water diversions, thereby violating our assumption of minimum impact.

The basins differ substantially in size (Table 1). In order to assess the effect of areal integration on the water balance residual, the water balance residual has been plotted versus basin area (Figure 8). This plot shows that as the size of the basin increases, the variability in water balance residual decreases, and the relative error in closing the water balance becomes negligible. The largest basin (308,210 km²; Mississippi river at Keokuk, Iowa) displays an average annual residual of only -5 mm, corresponding to -0.7 percent of the average annual basin precipitation. However, because the sample size diminishes as the basin area increases, this conclusion is tentative. Nevertheless, due to the apparent dependency of variability in water balance residual upon basin size, it was decided to restrict further statistical analyses of water balance residuals to basins of smaller size. The cutoff was arbitrarily set at 10,000 km², resulting in a basin subset of 120 basins.

Frequency histograms of the water balance residuals were constructed for the basin subset and the entire set of HUCs (Figure 9). Histograms are presented for residuals expressed in absolute units (mm) and in relative units (percentage of average annual basin precipitation). Summary statistics of the water balance residuals are presented in Table 2. The basin subset exhibits a slightly negative average annual residual of -7.7 mm, or -1.7 percent of average annual basin precipitation. The results for the entire set of component HUCs are similar, with an average annual residual of -5.5 mm, or -1.4 percent of average annual precipitation. All distributions are negatively skewed, with median values for the basin subset close to zero.

In order to determine whether there exist any relationships between the estimated water balance residual and components of the water balance or basin characteristics, additional analyses were carried out on the basin subset, relating the average annual water balance residual to: (1) average annual precipitation; (2) average annual precipitation minus streamflow; (3) average annual potential minus actual evapotranspiration; (4) average annual relative (actual as a fraction of potential) evapotranspiration; (5) 1985 annual groundwater withdrawal; and (6) mean basin elevation (Figure 10). Where applicable, simple linear regressions were performed for trend detection purposes. All results are presented for water balance residuals expressed in relative units (i.e., percentage of average annual precipitation).

Relating the water balance residual to precipitation (Figure 10a) indicates that, for precipitation values smaller than 900 mm, the water balance residual is negative and exhibits a positive correlation with precipitation ($r=0.53$, $p<0.05$). For precipitation values larger than 1100 mm, the water balance residual is independent of precipitation and close to zero. Because irrigated agriculture is often associated with areas of low precipitation, this trend could be a direct reflection of anthropogenic influences, i.e., through net groundwater withdrawals and net diversion of surface waters. The trend is more pronounced when relating the water balance residual to the value of precipitation minus streamflow (i.e., our independent water balance evapotranspiration estimate) (Figure 10b). For values of precipitation minus streamflow less than 750 mm, a positive correlation is apparent ($r=0.78$, $p<0.05$). This indicates that when basin evapotranspiration is small, the effect of an error in closure of the water balance increases.

The effect of the relative degree of soil control or climate control of evapotranspiration (i.e., effect of moisture availability) on water balance closure can be assessed by relating the water balance residual to the value of potential minus actual evapotranspiration (Figure 10c). For values of potential minus actual evapotranspiration less than 900 mm, the water balance residual exhibits a positive correlation ($r=0.72$, $p<0.05$), whereas for higher values there is relatively more scatter and no apparent relation. According to the complementary relationship (Figure 1), a similar, though reversed, behavior should then be observed when relating the water balance residual to the value of relative (i.e., actual as a fraction of potential) evapotranspiration. Figure 10d shows that the water balance residual indeed displays an apparent negative correlation with relative evapotranspiration for values of relative evapotranspiration exceeding 0.40 ($r=0.71$, $p<0.05$), whereas for lower values of relative evapotranspiration there is more scatter and no apparent correlation. These results indicate that the water balance residuals tend to become more negative when moving towards regions of increased climate control of evapotranspiration rates. Increased climate control in this context refers to increased moisture availability.

When evaluating the relation between residual and precipitation, it was suggested that the negative correlation could be a result of the effect of net groundwater withdrawals. Using USGS

water-use estimates [Solley *et al.*, 1988] we analyzed the effect of groundwater withdrawal on water balance residual. Figure 10e indicates that there is no clear relationship between groundwater withdrawal and water balance residual. Unfortunately the water use data only provides rough estimates, not necessarily based on actual measurements. Therefore no major conclusions can be drawn.

In the study area, continental scale precipitation displays an overall, climatological gradient, from a humid climate in the east to a semi-arid climate in the west. As continental scale elevation generally increases in a similar east-west direction, there is a strong negative correlation between precipitation and elevation. Thus, when comparing the water balance residual with mean basin elevation, one would expect a negative correlation between residual and elevation, as was indeed found (Figure 10f) ($r=0.40$, $p<0.05$).

4.3 Evapotranspiration-Precipitation Relational Analysis

The hypothesis of the complementary relationship in regional evapotranspiration is based on the interaction between the land surface and the atmosphere. The meteorological state of the atmosphere is a direct result of this feedback. Therefore, having contemporaneous observations of the meteorological variables is essential for estimating evapotranspiration. However, because there are few stations in our study area which record all the required meteorological variables, we spatially interpolated the meteorological variables prior to calculating the gridded evapotranspiration estimates. In this section, results are presented to test the implications of this approach.

Figure 1 presented the schematic representation of the complementary relationship in regional evapotranspiration. This scheme corresponds to the timestep of model application. A similar graphical relationship can be constructed using average annual values. Figure 11a presents the graphical relationship between average annual values of precipitation and actual, potential and wet environment evapotranspiration, as obtained from the basin subset results. Annual precipitation has been used as a surrogate for moisture availability. The values for precipitation and evapotranspiration are standardized by expressing them as a fraction of the wet environment

evapotranspiration. Apart from the CRAE evapotranspiration estimates, Figure 11a also includes the independent water balance estimate of actual evapotranspiration (i.e., precipitation less streamflow). The figure indicates that even on an average annual basis, there is a clear relationship between evapotranspiration and precipitation. This relationship is very similar to the general complementary relationship (Figure 1), except that, on an average annual basis, actual evapotranspiration does not approach its potential value for any of the basins analyzed, as expected. On the far right of this figure, a group of 5-6 basins can be distinguished, for which actual evapotranspiration estimates differ substantially from their independent water balance estimates. These basins are located in the northern portion of the Appalachian Mountains region (Maine).

Figure 11b presents a similar graphical relationship, derived from applying the CRAE model to the 1962-1988 monthly SAMSON meteorological station data [NREL, 1992]. Also here, the figure indicates a clear relationship between evapotranspiration and precipitation. Compared to the basin results, there is relatively more scatter.

The validity of calculating evapotranspiration with interpolated, non-contemporaneous observations of the meteorological variables was tested by comparing the basin subset results with the meteorological stations results. The comparison was based on their observed relationship between average annual values of precipitation and actual evapotranspiration. The results are presented in Figure 12. The iterative smoothing procedure LOWESS (locally weighted scatter-plot smoothing) [Cleveland, 1979] was applied to describe the relationship between evapotranspiration and precipitation, for both the basins results and the stations results. The LOWESS curves were used for exploratory analysis purposes, avoiding the necessity to assign one single functional relationship. Overall, the LOWESS curves are very similar, although sections can be identified where the curves are different. For standardized precipitation values between 0.3 and 0.8, the basin subset seems to slightly underestimate evapotranspiration. For values greater than 1.0, the basins subset seems to slightly overestimate actual evapotranspiration.

In addition, significance tests were carried out to determine whether the basin subset and stations results exhibit significantly different relationships between average annual precipitation and actual evapotranspiration. Least square fits of log-transformed linear functions were obtained for the basin subset and stations results. Significance tests ($\alpha = 0.05$) on the regression parameters (slope and intercept) of the resulting linear functions indicated that the regression parameters obtained for the basin subset results were not significantly different from the parameters obtained for the stations results. Both the basin subset and the stations results lead to the same relationship, thus validating our approach.

5. DISCUSSION AND CONCLUSION

The objective of this study was to evaluate the complementary relationship in regional evapotranspiration. The evaluation was based on comparing evapotranspiration estimates produced by Morton's CRAE model with independent estimates obtained from long-term large-scale water balances.

Based on analyses of spatial interpolation performance, we confined our study area to the region east of the Continental Divide. For the water years 1962-1988, monthly surfaces were constructed of meteorological variables, together with the resulting CRAE model evapotranspiration estimate. A total of 164 minimum impacted river basins were selected, comprising 25 percent coverage of the study area. For the selected basins, average annual water balance residuals were calculated as the difference between precipitation minus streamflow minus the CRAE model evapotranspiration estimate.

Average annual surfaces of wet environment evapotranspiration and potential evapotranspiration indicated gradients that are a result of gradients in radiative forcing and a combination of radiative and precipitation forcing, respectively. In the western part of the study area, regions were identified where, on an average annual basis, evapotranspiration exceeds precipitation. These

regions are generally associated with irrigated agriculture, groundwater depletion and/or surface water diversions. However, the spatial extent and magnitude of this precipitation deficit could be an indication that the evapotranspiration estimates produced by the CRAE model are too high. This can be attributed to either the CRAE model itself, or to the inappropriateness of the meteorological forcing fields (see below).

Results from the water balance residual analysis indicate an excellent performance of the CRAE model, as shown in Table 2. Average estimation errors (water balance residuals), when expressed as percent of average annual precipitation, were negative and generally small, with an average value of -1.7 percent. Water balance residuals are generally small in the Midwest and Coastal Plains (± 4 percent of average annual precipitation), but large, negative residuals were observed for the Appalachian Mountains range, especially northern Maine, and in the Northern Great Plains and southern Texas. As explained above, the negative residuals in the latter two regions may be the result of anthropogenic influences. Thus, for these regions it is very difficult to draw conclusions about the performance of the CRAE model, without excluding the validity of our basic assumptions of minimum impact, stationarity in climatic forcing and negligible net groundwater flow out of the basin. Especially the effect of groundwater pumping and surface water diversions may not have been adequately evaluated in this study because of data availability limitations.

Scatterplots of residual versus various variables indicated that the residuals tend to become more negative when moving into regions of low precipitation. This can be attributed to the effect of irrigated agriculture and other anthropogenic influences or to CRAE model performance. However, the residual also tends to become more negative when moving into regions of high moisture availability (i.e., high relative evapotranspiration). Because apparently no basic assumptions are violated, this suggests an over-prediction in CRAE model evapotranspiration for these regions.

The final results in this paper included general relationships between average annual values of evapotranspiration and precipitation. The observed relationships are very similar to the general complementary relationship. A group of basins was identified which displayed a substantially

different behavior. These basins are in the upper range of moisture availability (i.e., average annual relative evapotranspiration), which indicates that, for this region (northern Maine), the CRAE model produces poor estimates of evapotranspiration. Using monthly averaged data from contemporaneous observations of meteorological variables from weather stations, similar general relationships between evapotranspiration and precipitation were constructed. The good agreement between the basin results and the station results supports the validity of our approach in applying the complementary relationship on interpolated, non-contemporaneous data of atmospheric forcing.

When studying feedback mechanisms between the land surface and the atmosphere, sound use of observational data combined with modeling results is imperative. The question of appropriateness of the meteorological data therefore is an important issue. Unfortunately, in some regions the long-term meteorological observations are not representative of regional characteristics, since the weather stations are often located at airports. This effect is compounded when combining humidity observations from these stations with temperature observations from a higher resolution station network. The appropriate spatial interpolation of meteorological variables, especially at varying spatial resolutions, certainly is an issue that deserves more attention, though out of the scope of this study.

Although an independent, theoretical proof of the complementary relationship hypothesis has not been established as of yet, this study provides indirect evidence supporting its plausibility. However, it is important to mention that the observed performance of the CRAE model should not only be attributed to its basic, driving hypothesis, but also to Morton's choice of governing equations. Within this context LeDrew's statement "For long-term means its success must depend on calibration procedures ... and errors which are self-compensating in the long run" [LeDrew, 1979] should be kept in mind. Overall, the excellent performance of the CRAE model indicates that the model is a powerful tool for predicting regional evapotranspiration, while further enhancing the tremendous importance of the concept of the complementary relationship for hydro-meteorological applications.

APPENDIX A: POTENTIAL EVAPOTRANSPIRATION AND REGIONAL ADVECTION

Potential evapotranspiration and wet environment evapotranspiration can be estimated using information from both the energy budget and water vapor transfer, together with a conceptual relationship between potential evapotranspiration and regional advection. The energy budget can be written as

$$Q_n = H + \lambda ET_a, \quad (\text{A1})$$

where ET_a is actual evapotranspiration rate, Q_n is the net available energy; H is the sensible heat flux; and λ is the latent heat of vaporization.

The water vapor transfer can be written as

$$\lambda ET_a = f_T(e_s - e_a), \quad (\text{A2})$$

where f_T is a vapor transfer coefficient; e_s is the actual vapor pressure at the surface; and e_a is the actual vapor pressure of the overlying air.

Combining both energy budget and water vapor transfer, *Penman* [1948] derived the so-called combination equation for a free water surface, which takes the general form

$$\lambda ET_p = \frac{\Delta}{\Delta + \gamma} Q_n + \frac{\gamma}{\Delta + \gamma} E_a, \quad (\text{A3})$$

where Δ is the gradient of the saturation vapor pressure function; γ is the psychrometric constant; and E_a is the drying power of the air, defined by

$$E_a = f_T(e_a^\circ - e_a), \quad (\text{A4})$$

where e_a° is the saturation vapor pressure of the air.

For most applications, the net available energy Q_n is often approximated by neglecting changes in energy storage, biological energy expenditure, energy advection, and other terms, as

$$Q_n = R_n - G, \quad (\text{A5})$$

where R_n is net radiation; and G is the ground heat flux.

Potential evapotranspiration is essentially driven by the net available energy and by the vapor pressure deficit. For conditions where the surface is completely saturated, and advection is nil, potential evapotranspiration becomes entirely governed by the net available energy. This evapotranspiration estimate is often labeled as the equilibrium evaporation, a concept first introduced by *Slatyer and McIlroy* [1961].

However, conditions of no advection rarely occur, and a vapor pressure deficit nearly always exists. *Priestley and Taylor* [1972] found that the existence of this constantly present vapor pressure deficit is directly related to the net available energy. They developed an empirical

equation which describes evaporation under conditions of minimal advection, which takes the general form

$$\lambda ET_{pe} = \alpha_e \frac{\Delta}{\Delta + \gamma} Q_n, \quad (\text{A6})$$

where the subscript *pe* stands for partial equilibrium. The coefficient α_e was determined through regression analysis. Combining several data sets from both saturated land surfaces and water surfaces, they obtained an average value of 1.26. Analytical expressions have been derived recently by *Eichinger et al.* [1996] and *Lhomme* [1997], supporting Priestley and Taylor's empirical findings.

Both the CRAE model and the Advection-Aridity model are based on the described concept of potential evapotranspiration and regional advection. Potential evapotranspiration is estimated using a combination of the energy budget and vapor transfer equations, while wet environment evapotranspiration is based on the Priestley-Taylor equation.

APPENDIX B: EQUATIONS CRAE MODEL

This section covers general computational specifics of the CRAE model. A detailed description can be found in *Morton* [1983].

Potential Evapotranspiration

In order to derive the combination equation in closed form, *Penman* [1948] assumed the surface temperature to be equal to the air temperature. Taking into account a possible disparity between air temperature and surface temperature at potential conditions, *Kohler and Parmele* [1967] adapted the combination equation, by incorporating a first-order Taylor expansion of the back radiation term in the energy budget, as follows

$$\lambda ET_p = \frac{\Delta(Q_n - \varepsilon\sigma T_a^4) + E_a(\gamma + 4\varepsilon\sigma T_a^3 f_T^{-1})}{\Delta + \gamma + 4\varepsilon\sigma T_a^3 f_T^{-1}}, \quad (\text{B1})$$

where ε is the surface emissivity; and σ is the Stefan-Boltzmann constant.

Morton [1983] followed *Kohler and Parmele's* approach in expanding the back radiation term, but evaluated the slope of the saturation vapor pressure function at the unknown surface temperature instead of at air temperature. Especially in arid regions, *Morton's* modification results in evapotranspiration estimates significantly different from *Kohler and Parmele's* approach [*L.H.J.M. Claessens*, unpublished data, 1997]. Due to *Morton's* modification, the combined energy budget and vapor transfer equations can not be expressed in a closed-form combination equation, thus requiring the use of an iterative scheme to solve for the surface temperature. The energy budget is formulated as

$$Q_n - 4\varepsilon\sigma T_s^3(T_s - T_a) = \gamma f_T(T_s - T_a) + \lambda ET_p \quad (\text{B2})$$

and the vapor transfer as

$$\lambda ET_p = f_T(e_s^* - e_a), \quad (\text{B3})$$

where e_s^* is the saturation vapor pressure at the surface. Combining both equations, the iteration involves the calculation of a surface temperature correction (δT_s) as

$$\delta T_s = \frac{Q_n - 4\epsilon\sigma T_a^3(T_s' - T_a) - \gamma f_T(T_s' - T_a) - f_T(e_s'^* - e_a)}{\Delta_s' f_T + \gamma f_T + 4\epsilon\sigma T_a^3}, \quad (\text{B4})$$

where Δ_s' is the slope of the saturation vapor pressure function; and $e_s'^*$ is the saturation vapor pressure, both evaluated at the trial surface temperature T_s' .

Wet Environment Evapotranspiration

Morton [1983] adapted the Priestley and Taylor [1972] equation, as to account for large-scale advection during seasons of low radiation and the possible disparity between surface temperature and air temperature at potential conditions. Wet environment evapotranspiration is calculated as

$$\lambda ET_w = b_1 + b_2 \frac{\Delta_s}{\Delta_s + \gamma} [R_n - 4\epsilon\sigma T_a^3(T_s - T_a)], \quad (\text{B5})$$

where b_1 and b_2 are coefficients with values of 14 Wm^{-2} and 1.20 , respectively. Morton obtained these coefficients and a vapor transfer related coefficient, f_z , through a global calibration using data for arid regions. Since under extreme arid conditions actual evapotranspiration is negligible, potential evapotranspiration equals twice wet environment evapotranspiration, thus enabling a direct calibration of the model coefficients.

Supporting Equations

The vapor transfer coefficient is wind-independent and is calculated as

$$f_T = \left(\frac{P_o}{P} \right)^{0.5} f_z \zeta^{-1}, \quad (\text{B6})$$

where P is atmospheric pressure; P_o is atmospheric pressure at sea level; f_z is a coefficient of value $28.0 \text{ Wm}^{-2} \text{ mbar}^{-1}$ or $32.2 \text{ Wm}^{-2} \text{ mbar}^{-1}$ for below freezing; and ζ is the stability factor, calculated as

$$\zeta^{-1} = 0.28 \left(1 + \frac{e_a}{e_a^o} \right) + \frac{\Delta R_n}{\gamma \left(\frac{P_o}{P} \right)^{0.5} f_z (e_a^o - e_a)}. \quad (\text{B7})$$

Saturation vapor pressure e^o (mbar) at temperature T ($^{\circ}\text{C}$) is calculated as

$$e^{\circ} = \begin{cases} 6.11 \exp\left(\frac{21.88T}{T + 265.5}\right) & T < 0^{\circ}C \\ 6.11 \exp\left(\frac{17.27T}{T + 237.3}\right) & T \geq 0^{\circ}C \end{cases} \quad (B8)$$

The slope of the saturation vapor pressure function is obtained by taking the derivative of the previous equations as follows

$$\Delta = \begin{cases} \frac{5809e^{\circ}}{(T + 265.5)^2} & T < 0^{\circ}C \\ \frac{4098e^{\circ}}{(T + 237.3)^2} & T \geq 0^{\circ}C \end{cases} \quad (B9)$$

ACKNOWLEDGMENTS

This work was partially supported by the Rocky Mountain Research Station of the U.S. Forest Service and the U.S. Department of Energy National Institute for Global Environmental Change. In addition, one of the co-authors (Jorge A. Ramírez) received partial support from the Colorado Water Resources Research Institute.

REFERENCES

- Ben-Asher, J. Estimating evapotranspiration from the Sonoita Creek watershed near Patagonia, Arizona. *Water Resour. Res.*, 17(4): 901-906, 1981.
- Bouchet, R.J. Evapotranspiration réelle et potentielle, signification climatique. *Int. Assoc. Sci. Hydrol.*, Proceedings, Berkeley, Calif., Symp. Publ. 62: 134-142, 1963.
- Brutsaert, W., and H. Stricker. An advection-aridity approach to estimate actual regional evapotranspiration. *Water Resour. Res.*, 15(2): 443-450, 1979.
- Calder, I.R. What are the limits on forest evaporation? - A further comment. *J. Hydrol.*, 89: 33-36, 1986.
- Chiew, F.H.S., and T.A. McMahon. The applicability of Morton's and Penman's evapotranspiration estimates in rainfall-runoff modeling. *Water Resour. Bul.*, 27(4): 611-620, 1991.
- Claessens, L. *The complementary relationship in regional evapotranspiration and long-term large-scale water budgets*. M.S. Thesis, Colorado State University, Fort Collins, Colorado, U.S.A. 159 pp. , 1996.
- Cleveland, W.S. Robust locally weighted regression and smoothing scatterplots. *J. Am. Stat. Assoc.*, 74: 829-836, 1979.

- Daly, C., R.P. Neilson, and D.L. Phillips. A statistical-topographic model for mapping climatological precipitation over mountainous terrain. *J. Appl. Meteor.*, 33: 140-158, 1994.
- Dolph, J., and D. Marks. Characterizing the distribution of observed precipitation and runoff over the continental United States. *Climatic Change*, 22: 99-119, 1992.
- Dooge, J.C.I. Hydrologic models and climate change. *J. of Geophys. Res.*, 97(D3): 2677-2686, 1992.
- Doyle, P. Modeling catchment evaporation: An objective comparison of the Penman and Morton approaches. *J. Hydrol.*, 12: 257-276, 1990.
- Eichinger, W.E., M.B. Parlange and H. Stricker. On the concept of equilibrium evaporation and the value of the Priestley-Taylor coefficient. *Water Resour. Res.*, 32(1): 161-164, 1996.
- Granger, R.J. A complementary relationship approach for evaporation from nonsaturated surfaces. *J. Hydrol.*, 111: 31-38, 1989.
- Granger, R.J., and D.M. Gray. Examination of Morton's CRAE model for estimating daily evaporation from field-sized areas. *J. Hydrol.*, 120: 309-325, 1990.
- Gutman, G.A. simple method for estimating monthly mean albedo of land surfaces from AVHRR data. *J. Appl. Meteor.*, 27(9): 973-988, 1988.
- Kim, C.P., and D. Entekhabi. Examination of two methods for estimating regional evaporation using a coupled mixed layer and land surface model. *Water Resour. Res.*, 33(9): 2109-2116, 1997.

- Kohler, M.A., and L.H. Parmele. Generalized estimates of free-water evaporation. *Water Resour. Res.*, 3(4): 997-1005, 1967.
- Kovacs, G. Estimation of average areal evapotranspiration - proposal to modify Morton's model based on the complementary character of actual and potential evapotranspiration. *J. Hydrol.*, 95: 227-240, 1987.
- LeDrew, E.F. A diagnostic examination of a complementary relationship between actual and potential evapotranspiration. *J. Appl. Meteorol.*, 18: 495-501, 1979.
- Lemur, R., and L. Zhang. Evaluation of three evapotranspiration models in terms of their applicability for an arid region. *J. Hydrol.*, 114: 395-411, 1990.
- Lhomme, J.-P. A theoretical basis for the Priestley-Taylor coefficient. *Boundary Layer Meteorol.*, 82: 179-191, 1997.
- McNaughton, K.G., and T.W. Spriggs. An evaluation of the Priestley and Taylor equation and the complementary relationship using results from a mixed-layer model of the convective boundary layer. *Estimation of areal evapotranspiration*. IAHS, Publ. No. 177: 89-104, 1989.
- Mooty, W.S., and H.H. Jeffcoat. *Inventory of inter basin transfer of water in the eastern United States*. U.S. Geological Survey, open-file report 86-148, 1986.
- Morton, F.I. Potential evaporation and river basin evaporation. *J. Hydraul. Div.*, ASCE, 91(HY6): 67-97, 1965.

- Morton, F.I. Operational estimates of areal evapotranspiration and their significance to the science and practice of hydrology. *J. Hydrol.*, 66: 1-76, 1983.
- Morton, F.I., F. Ricard, and S. Fogarasi. *Operational estimates of areal evapotranspiration and lake evaporation - Program CRAE*. National Hydrology Research Institute, Paper No. 24, Ottawa, Canada. 75 pp. , 1985.
- Nash, J.E. Potential evaporation and "the complementary relationship". *J. Hydrol.*, 111: 1-7, 1989.
- NREL. *User's Manual for National Solar Radiation Data Base (1961-1990)*. National Renewable Energy Laboratory, Golden, Colorado, U.S.A. 93 pp. , 1992.
- Parlange, M.B., and G.G. Katul. Estimation of the diurnal variation of potential evaporation from a wet bare soil surface. *J. Hydrol.*, 132: 71-89, 1992a.
- Parlange, M.B., and G.G. Katul. An advection-aridity evaporation model. *Water Resour. Res.*, 28(1): 127-132, 1992b.
- Penman, H.L. Natural evaporation from open water, bare soil and grass. *Proc. Roy. Soc. London*, A193: 120-146, 1948.
- Petsch, H.E. Jr. *Inventory of inter basin transfer of water in the western conterminous United States*. U.S. Geological Survey, open-file report 85-166, 1985.
- Priestley, C.H.B., and R.J. Taylor. On the assessment of surface heat flux and evaporation using large scale parameters. *Mon. Weath. Rev.*, 100: 81-92, 1972.

Sharma, T.C. An evaluation of evapotranspiration in tropical central Africa. *Hydrol. Sci. J.*, 33(2): 31-40, 1988.

Slack, J.R., and J.M. Landwehr. *Hydro-climatic data network (HCDN): A U.S. Geological Survey streamflow data set for the United States for the study of climate variations, 1874-1988*. U.S. Geological Survey, open-file report 92-129, 1992.

Slatyer, R.O., and I.C. McIlroy. *Practical climatology*. CSIRO, Melbourne, Australia. 310 pp, 1961.

Solley, W.B., C.F. Merk and R.R. Pierce. *Estimated use of water in the United States in 1985*. U.S. Geological Survey, circular 1004. 82 pp. , 1988.

Wallis, J.R., D.P. Lettenmaier, and E.F. Wood. A daily hydroclimatological data set for the continental United States. *Water Resour. Res.*, 27(7): 1657- 1663, 1991.

FIGURE CAPTIONS

- Figure 1. Schematic representation of the complementary relationship in regional evapotranspiration (assumes constant energy availability).
- Figure 2. Spatial distribution of the difference in IDW-generated and PRISM-generated precipitation surfaces, expressed in (a) mm; and (b) percentage of PRISM. See text for explanation.
- Figure 3. Probability distribution plots of error induced by resolution of spatial interpolation. (a) Precipitation. (b) Actual evapotranspiration.
- Figure 4. Location of selected basins.
- Figure 5. Average annual surfaces of (a) wet environment evapotranspiration; (b) potential evapotranspiration; (c) actual evapotranspiration; and (d) precipitation.
- Figure 6. Average annual surface of the difference between precipitation and actual evapotranspiration, expressed in (a) mm; and (b) percentage of average annual precipitation.
- Figure 7. Spatial distribution of water balance residual, expressed in (a) mm; and (b) percentage of average annual precipitation.
- Figure 8. Average annual water balance residual versus basin area. Water balance residual expressed in (a) mm; and (b) percentage of average annual precipitation.

Figure 9. Frequency histogram of water balance residual. For basins smaller than 10,000 km², expressed in (a) mm; and (b) percentage of average annual precipitation. For the component HUCs, expressed in (c) mm; and (d) percentage of average annual precipitation.

Figure 10. Average annual water balance residual versus: (a) average annual precipitation; (b) average annual precipitation minus streamflow; (c) average annual potential minus actual evapotranspiration; (d) average annual relative evapotranspiration; (e) average annual groundwater withdrawal; and (f) mean basin elevation. Analyses performed for basins smaller than 10,000 km². Water balance residual expressed as percentage of average annual precipitation.

Figure 11. Relationship between average annual values of precipitation and actual, potential and wet environment evapotranspiration, as obtained from: (a) basin subset results; and (b) meteorological station results. Evapotranspiration and precipitation expressed as a ratio of wet environment evapotranspiration. See text for explanation.

Figure 12. Comparison of relationship between average annual values of precipitation and actual evapotranspiration, comparing basin subset results versus meteorological station results. Evapotranspiration and precipitation expressed as a ratio of wet environment evapotranspiration. See text for explanation.

Table 1. Classification of selected basins by size

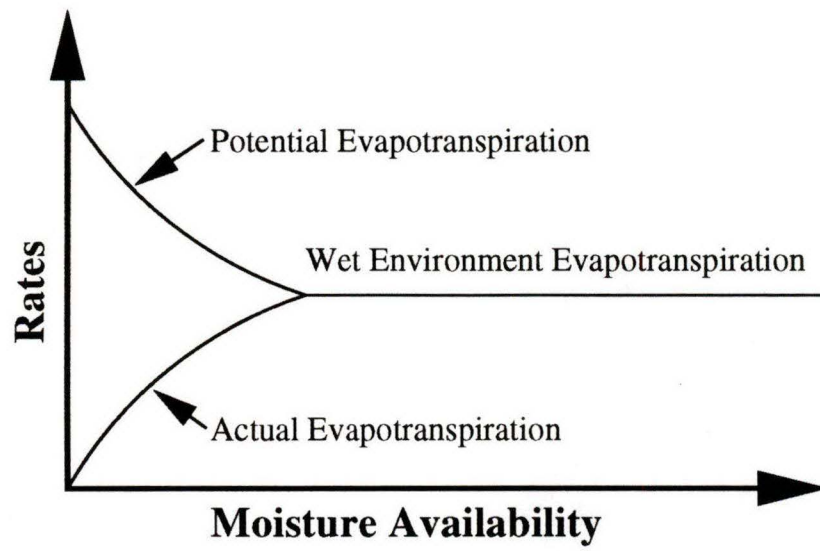
Basin Area [km ²]			number
0	-	5,000	81
5,000	-	10,000	39
10,000	-	20,000	23
20,000	-	40,000	14
40,000	-	100,000	5
	>	100,000	2

Total			164

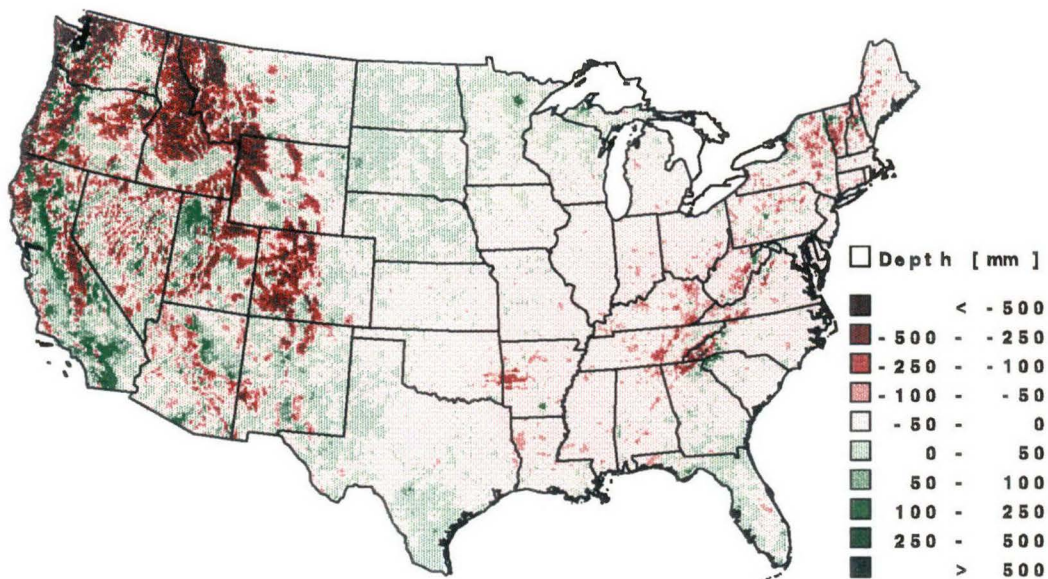
Table 2. Summary statistics of water balance residual for river basin subset (< 10,000 km²) and 8-digit hydrologic units

	Mean	Median	Stdv.	Skew.	Min.	Max.
Basin Subset						
[mm]	-7.70	-0.98	58.67	-1.02	-223.22	94.36
[% prcp]	-1.68	-0.12	7.35	-0.75	-24.31	18.23
Hydrologic Units						
[mm]	-5.53	-6.30	49.10	-2.04	-306.22	94.36
[% prcp]	-1.43	-0.47	6.52	-2.32	-41.16	18.23

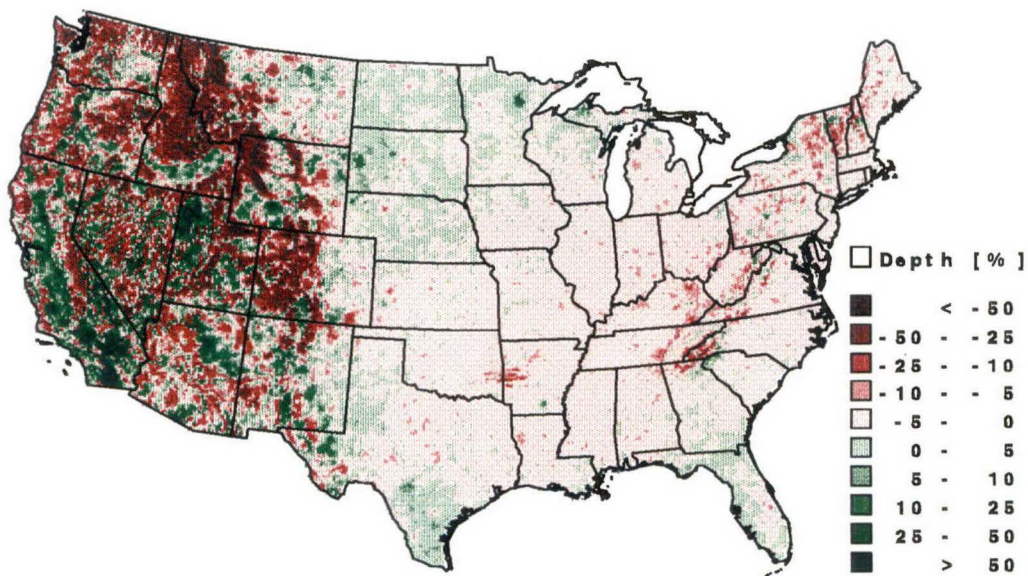
Residual is presented in absolute units (mm) and in relative units (percentage of average annual basin precipitation)

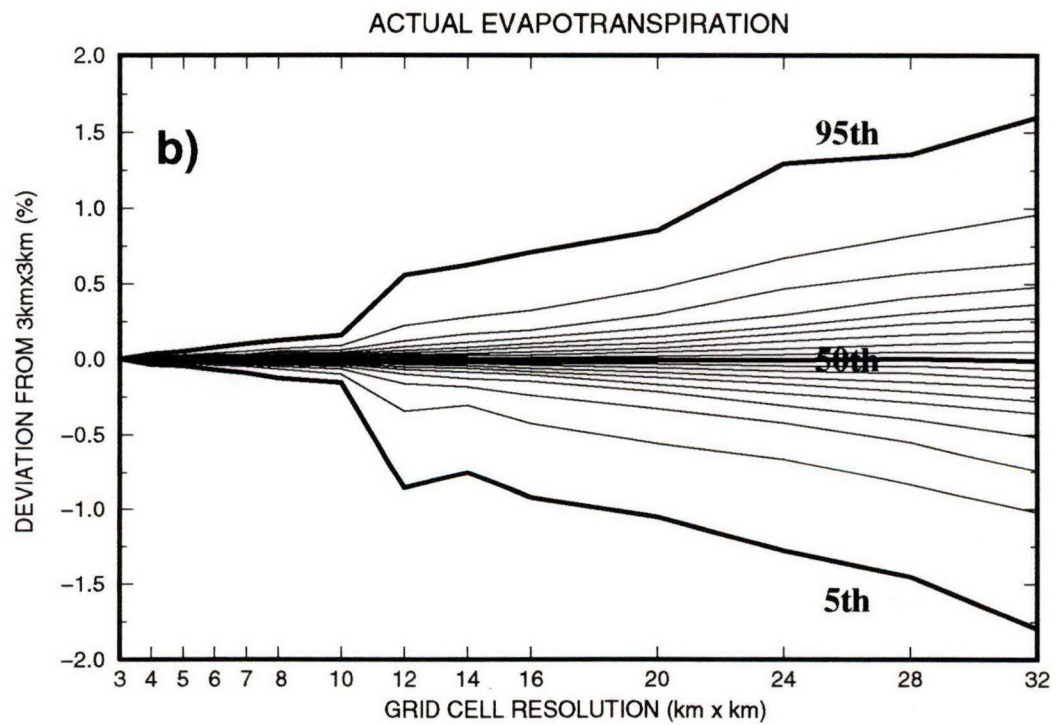
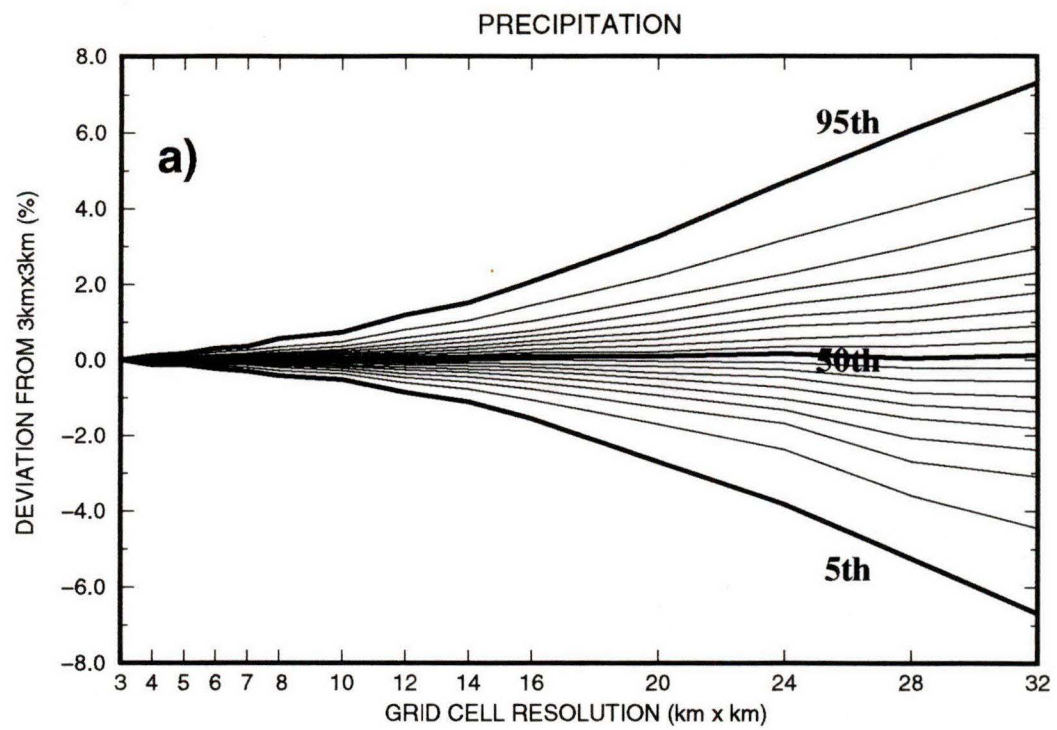


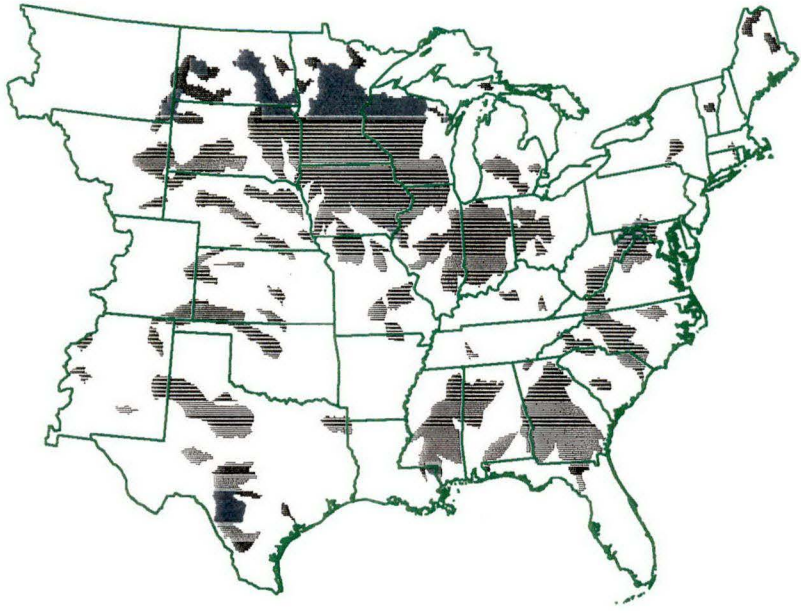
IDW versus PRISM [mm]



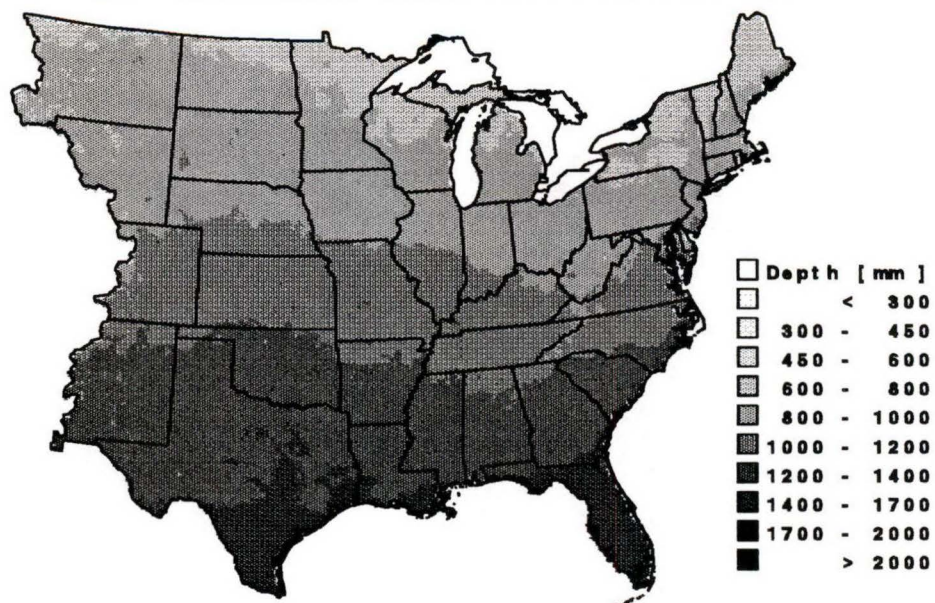
IDW versus PRISM [%]



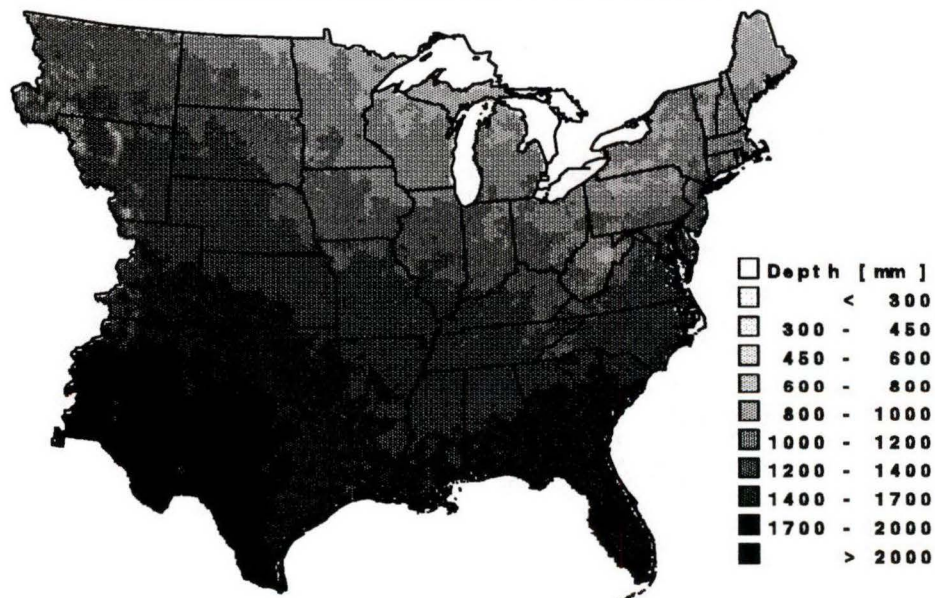




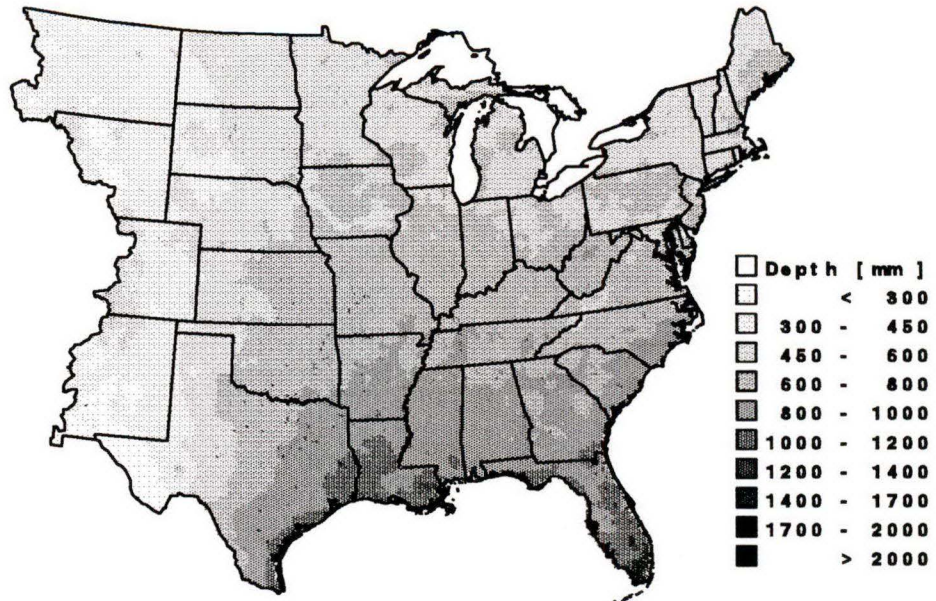
WET ENVIRONMENT EVAPOTRANSPIRATION



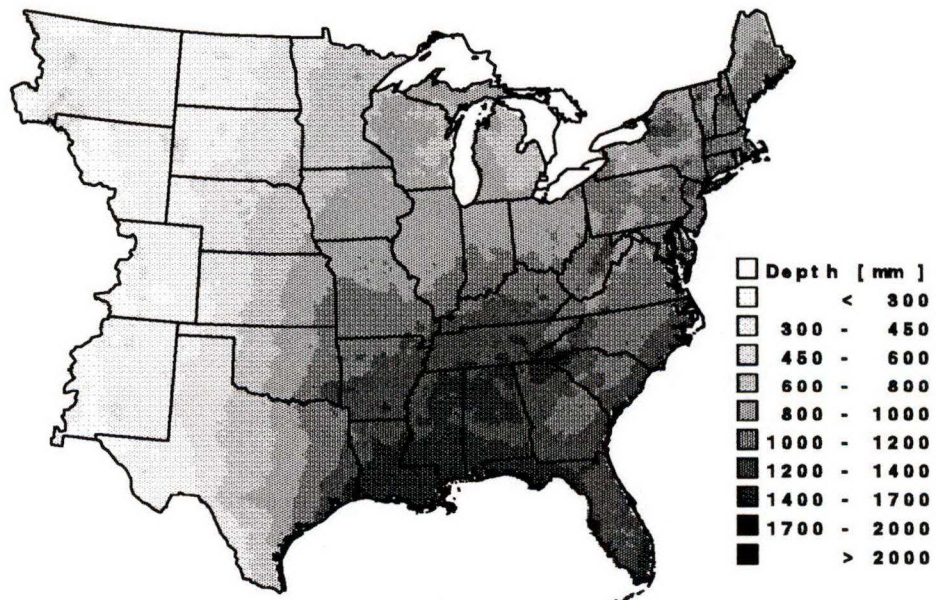
POTENTIAL EVAPOTRANSPIRATION



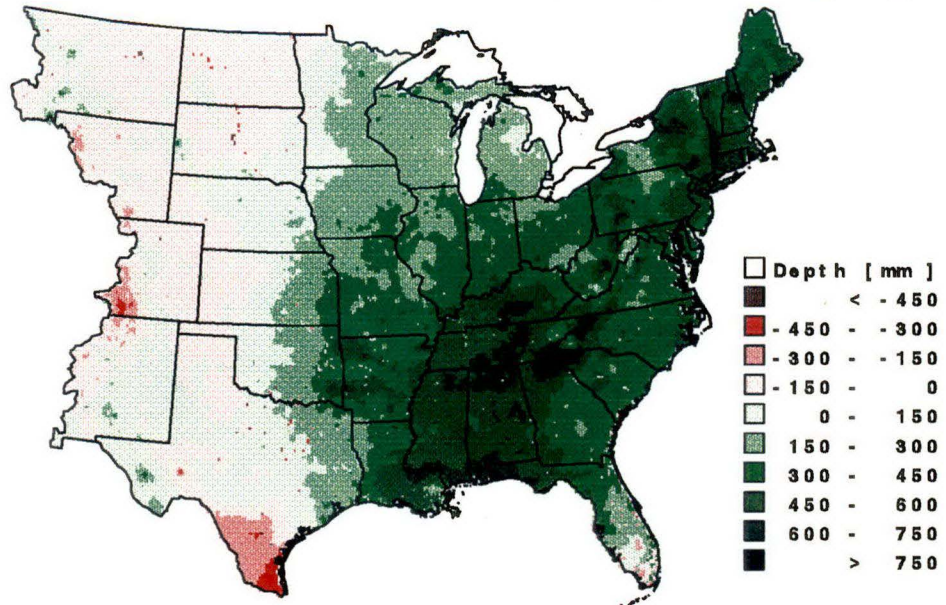
ACTUAL EVAPOTRANSPIRATION



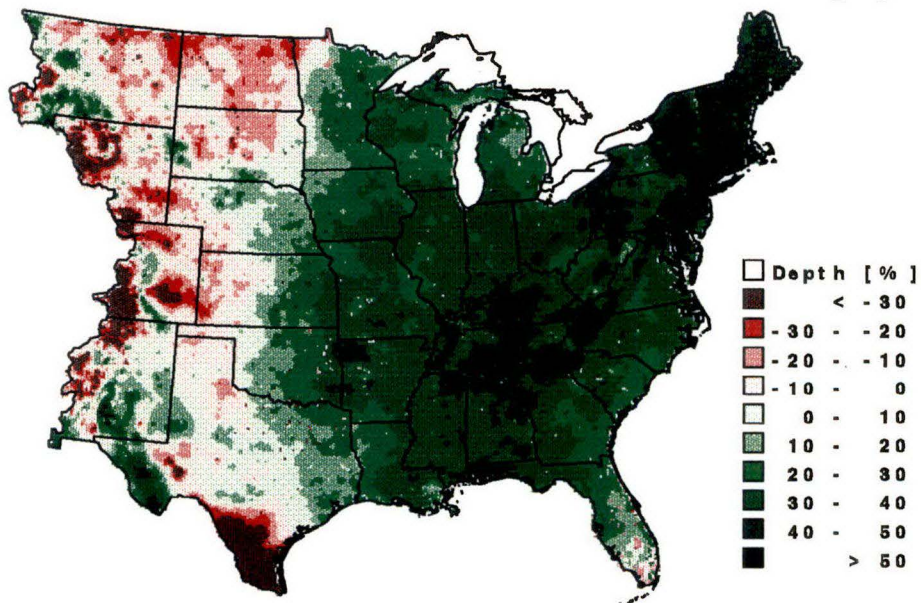
PRECIPITATION

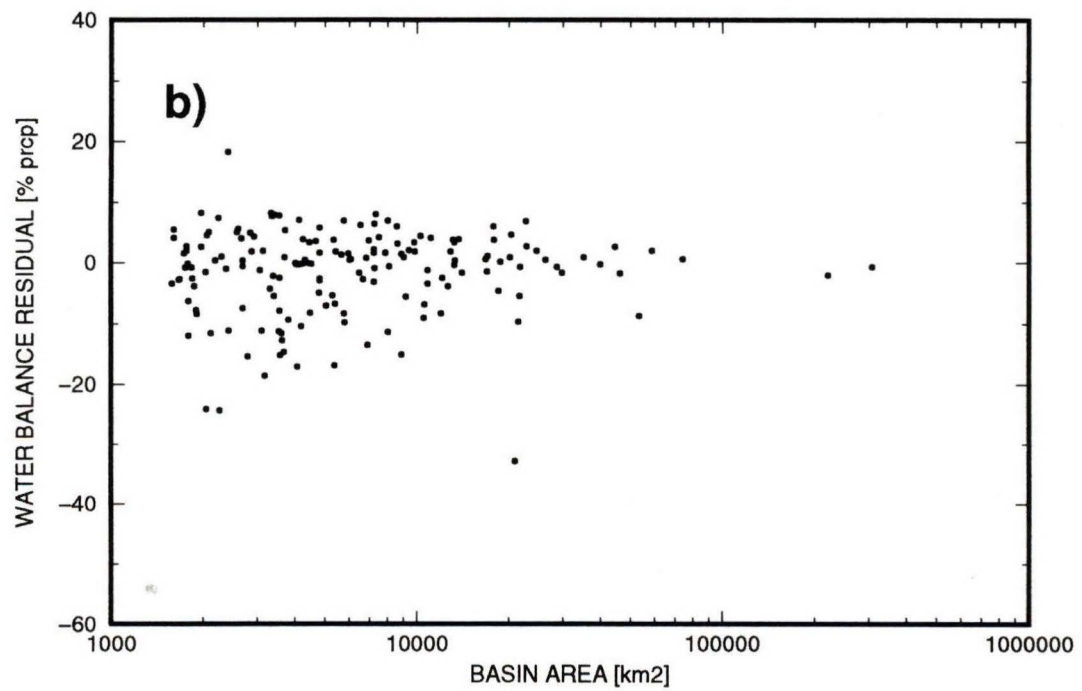
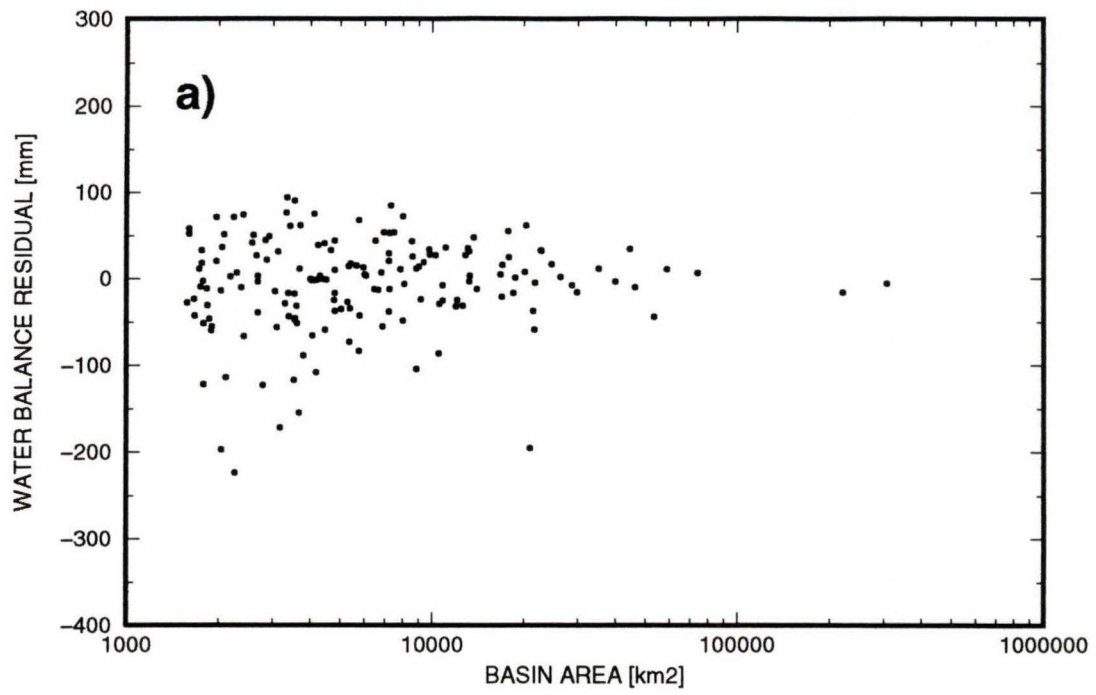


PRECIPITATION MINUS EVAPOTRANSPIRATION [mm]

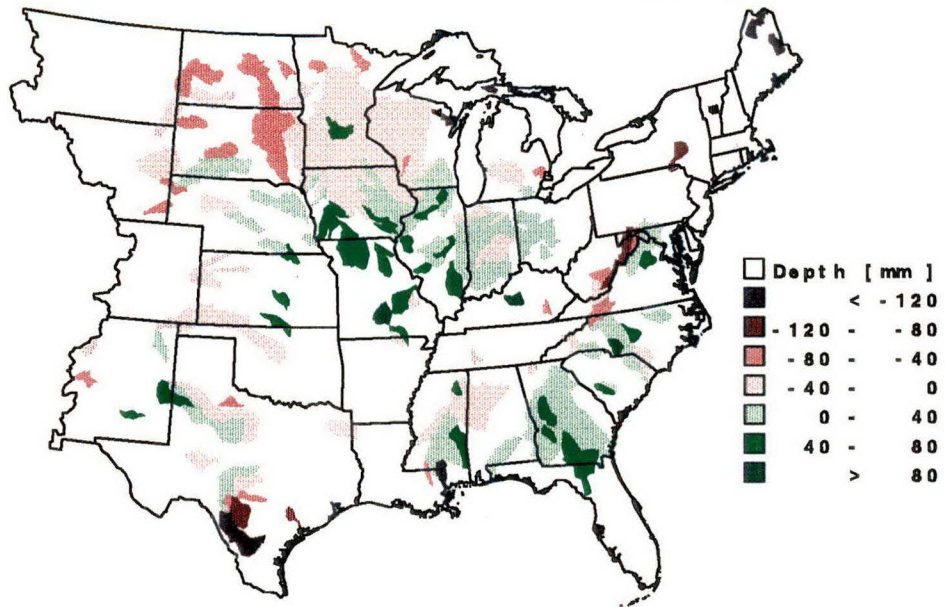


PRECIPITATION MINUS EVAPOTRANSPIRATION [%]

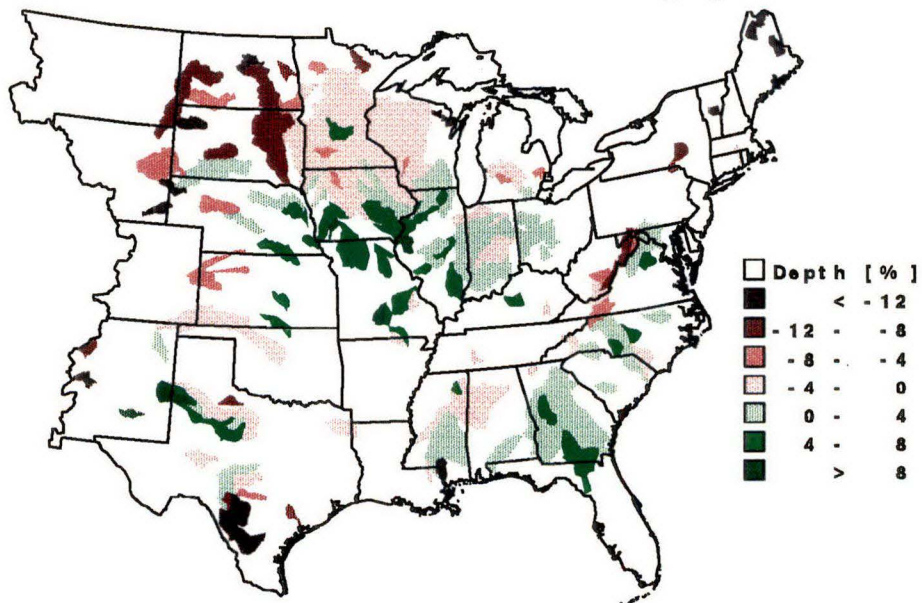




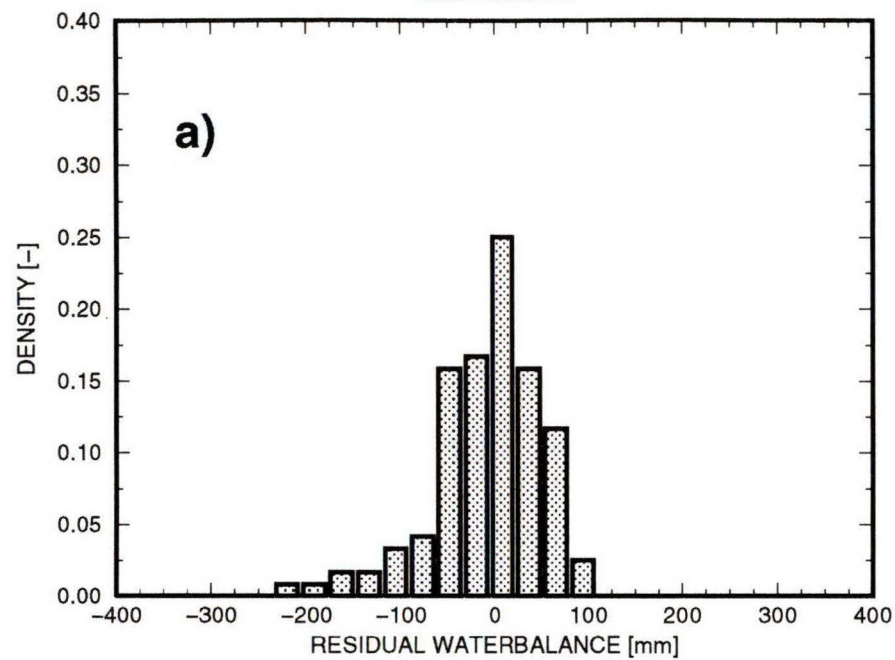
WATER BALANCE RESIDUAL [mm]



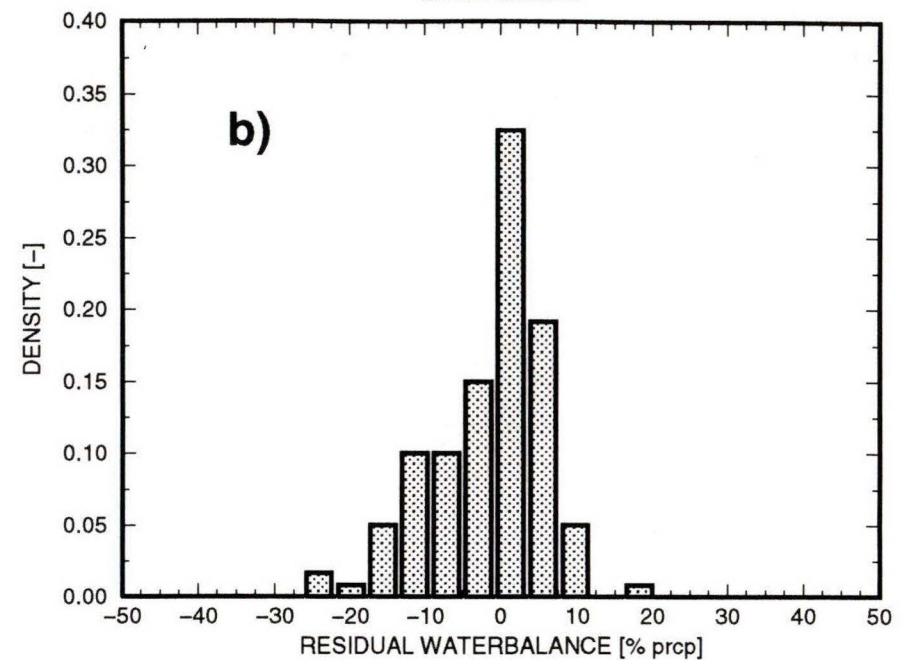
WATER BALANCE RESIDUAL [%]



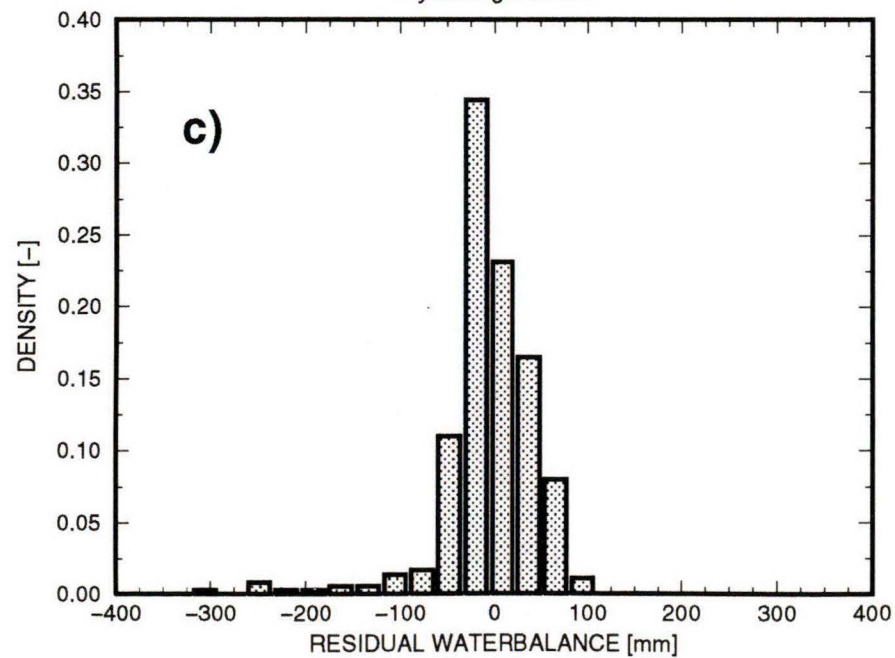
Basin Subset



Basin Subset



Hydrologic Units



Hydrologic Units

